ORIGINAL RESEARCH

Expression and significance of the Hedgehog signal transduction pathway in oxygen-induced retinal neovascularization in mice

Meilin Liu
Xiaolong Chen
Henan Liu
Yu Di

Department of Ophthalmology,
Shengjing Affiliated Hospital, China
Medical University, Shenyang, Liaoning,
People's Republic of China

Aim: The aim of the study was to investigate the signal transduction mechanism of Hedgehog–vascular endothelial growth factor in oxygen-induced retinopathy (OIR) and the effects of cyclopamine on OIR.

Methods: An OIR model was established in C57BL/6J mice exposed to hyperoxia. Two hundred mice were randomly divided into a control group, an OIR group, an OIR-control group (treated with isometric phosphate-buffered saline by intravitreal injection), and a cyclopamine group (treated with cyclopamine by intravitreal injection), with 50 mice in each group. The retinal vascular morphology was observed using adenosine diphosphatase and number counting using hematoxylin and eosin-stained image. Quantitative real-time quantitative polymerase chain reaction was used to detect mRNA expression. Protein location and expression were evaluated using immunohistochemistry and Western blot.

Results: The OIR group and OIR-control group demonstrated large-area pathological neovascularization and nonperfused area when compared with the control group (both $P<0.05$). The area of nonperfusion and neovascularization in the cyclopamine group was significantly reduced compared with the OIR and OIR-control groups (both $P<0.05$). Compared with the control group, the OIR and OIR-control groups had more vascular endothelial cells breaking through the inner limiting membrane. The number of new blood vessel endothelial cell nuclei in the cyclopamine group was significantly reduced (both $P<0.05$) when compared with the OIR and OIR-control groups. The mRNA and protein expressions of Smoothened, Gli1, and vascular endothelial growth factor in the signal pathway of the OIR and OIR-control groups were significantly higher than those of the control group; however, in the cyclopamine group, these factors were reduced when compared with the OIR and OIR-control groups (all $P<0.05$).

Conclusion: Our data suggest that abnormal expression of the Hedgehog signaling pathway may be closely associated with the formation of OIR. Inhibiting the Smoothened receptor using cyclopamine could control retinal neovascularization, providing new ideas and measures for the prevention of oxygen-induced retinal neovascularization.

Keywords: Hedgehog signaling pathway, neovascularization, oxygen-induced retinopathy, retinopathy of prematurity, cyclopamine

Correspondence: Xiaolong Chen
Department of Ophthalmology,
Shengjing Affiliated Hospital, China
Medical University, 36 Sanhao Street,
Heping, Shenyang, Liaoning 110004,
People's Republic of China
Email chenxiaolong_sj@163.com

Introduction

Retinopathy of prematurity (ROP) is a vasoproliferative retinal disorder unique to premature infants.[1] It is characterized by retinal ischemia, neovascularization, and proliferative retinopathy that can lead to a retinal detachment and permanent blindness. There are many pathways and factors involved in the regulation of ROP formation, but the specific pathogenesis is not yet clear.

In 1980, when the Hedgehog gene was first discovered in Drosophila, researchers discovered that when a gene mutation occurs, numerous thorns form on fruit fly larvae, in a manner similar to a hedgehog, for which this pathway was named.[2] The Hedgehog signaling pathway consists of the ligand, Hedgehog (Hh); membrane protein receptor, Patched (Ptc); Smoothened (Smo); glioblastoma transcription factor, Gli; and downstream target genes. The researchers confirmed that the Hedgehog signaling pathway is highly conserved in vertebrates and invertebrates and has an important role in the growth and development of many organisms. However, few studies have investigated the role of Hedgehog signal transduction pathway in ROP. We created an experimental mouse model of oxygen-induced retinopathy (OIR) to simulate the occurrence of ROP, which was induced by hyperoxia, to observe the expressions of Smo and Gli1, as well as key factors in the Hedgehog signaling pathway; to evaluate the Hedgehog signaling pathway relationship with vascular endothelial growth factor (VEGF), the main factor of retinal neovascularization (RNV); and to explore the effect of inhibition of the Hedgehog signaling receptor, Smo, on RNV, providing new ideas for the prevention and treatment of retinal vascular diseases.

Materials and methods
Animals and groups
All experimental animals, operations, and experimental conditions were performed in accordance with the relevant provisions of the "Regulations on the administration of laboratory animals" promulgated by the National Science and Technology Commission of the People's Republic of China. The animal experiments were approved by the ethics committee of Shengjing Affiliated Hospital, China Medical University (ethics number: 2015PS214K). Two hundred 7-day-old, specific-pathogen-free C57BL/6J mice were provided by the Beijing Huafukang Biological Technology Co Ltd. The animals' feeding environment was kept at 23°C±2°C with indoor fluorescent lighting (12-h light–dark cycle), and lactating mice were exchanged every 2 days.

Using a random number table method, the mice were divided into a control group, an OIR group, an OIR-control group, and a cyclopamine group, with 50 mice in each group. The mice in the control group were raised along with lactating mice until they were 17 days old under normal conditions. According to Smith et al's method,[3] the 7-day-old mice in the OIR group, OIR-control group, and inhibitor group were placed in an airtight glass box with an oxygen volume fraction of 75%±2% along with lactating mice for 5 days before returning them to normal air. Then, 12-day-old mice in the OIR group and cyclopamine group were administered

an intravitreal injection of 1 µL of phosphate buffer saline (PBS) and 0.8 mg/mL of cyclopamine solution into right eyes, respectively. All experimental mice were sacrificed at 17 days of age and their right eyes were used as experimental tissue.

Angiography using adenosine diphosphatase
From each group, ten 17-day-old mice were randomly selected; 10% chloral hydrate intraperitoneal anesthesia and left ventricular perfusion with a 4% polyformaldehyde solution for approximately 5 min were performed, and the eyes were enucleated and fixed for 1 h. Anterior ocular segment was removed and retina was cut into four or five flaps. Retinas were rinsed with TRIS maleic acid buffer (4°C, pH =7.2, 50 mmol/L) for five times (15 min each time). The retinas were then transferred into freshly prepared TRIS maleic acid buffer (37°C, pH =7.2, 0.2 mol/L, containing lead nitrate 3 mmol/L, magnesium chloride 6 mmol/L, ADP 1 mg/mL) for 15 min. Then, the retinas were rinsed with TRIS maleic acid buffer (20°C, pH =7.2, 50 mmol/L) for five times (15 min each time). Then, 1:10 ammonium sulfide was added to color. After rinsing with TRIS maleic acid buffer, retinas were sealed with glycerin gelatin. The retinas were observed and photographed under optical microscope. Image-Pro plus 6.0 software was used to count neovascularization, nonperfused area, and the total retinal area.

H&E staining
From each group, ten 17-day-old mice were randomly selected. Each eye was embedded in paraffin after treatment with 4% paraformaldehyde. Examination of 3.5-µm paraffin-processed cross-sections of mouse eyes was performed, and from each eye, 10 pieces were selected for staining (Xylene-I for 10 min→Xylene-II for 5 min→100% ethanol-I for 3 min→100% ethanol-II for 2 min→95% ethanol for 2 min→80% ethanol for 2 min→wash away ethanol→hematoxylin for 10 min→water flush for 10 min→eosin for 1 min→80% ethanol for 1 min→95% ethanol for 1 min→100% ethanol-I for 1 min→100% ethanol-II for 1 min→Xylene-I for 2 min→Xylene-II for 2 min). Images were captured under a microscope (B201; Olympus, Tokyo, Japan). The number of endothelial cell nuclei in the retinal inner limiting membrane (ILM) was counted using a double-blind method.

Immunohistochemistry
We used a biotin-streptavidin HRP detection system (SP-9000; Beijing Zhongshan Jinqiao Biotechnology Co., Ltd., Beijing, People's Republic of China) to perform immunohistochemistry. Formalin-fixed, paraffin-embedded eye tissue sections

(3.5 µm thick) were placed on slides, deparaffinized in xylene, and rehydrated by incubation in graded ethanol baths in PBS. Endogenous peroxidase was blocked with hydrogen peroxide. The sections were then treated with goat serum for 30 min and incubated overnight with the following antibodies: rabbit anti-Smo polyclonal antibody (1:50 dilution; ab72130; Abcam, Cambridge, UK), rabbit anti-Gli1 polyclonal antibody (1:50 dilution; sc-20687; Santa, Santa Cruz, CA, USA), mouse anti-VEGF monoclonal antibody (1:100 dilution; sc-7269; Santa, USA) at 4°C. Subsequently, they were incubated with Biotin-labeled goat anti-rabbit/ mouse IgG secondary antibodies (SP-9000; Zhongshan Jinqiao Biotechnology Co., Ltd., Beijing, People's Republic of China) for 15 min at room temperature. The primary antibody was replaced with PBS for the negative controls, and 3,3′-diaminobenzidine was used as the chromogen. The images were observed and captured using an Olympus B201 optical microscope (Olympus, Tokyo, Japan).

Real-time polymerase chain reaction (RT-qPCR)

Total retinal RNA was extracted with TRIzol (Invitrogen, Carlsbad, CA, USA). The RNA purity was determined using absorbance at 260 and 280 nm (A260/280) using multifunctional enzyme labeling instrument (Synergy H1; BioTek, Winooski, VT, USA). RT-qPCR amplification was performed using a reverse transcription kit (PrimeScript™ RT Reagent kit with gDNA Eraser; RR420A; Takara Bio, Otsu, Japan) after cDNA synthesis (SYBR@ Premix ExTaq™; RR047A; Takara Bio). Primers were designed by and purchased from Sangon Biotech Co Ltd (Shanghai, People's Republic of China). β-actin was used as a normalized control. The mRNA levels of Smo (primers: 5′-GATGTGTCCGTTACCCCTGT-3′ and 5′-CCTCTTCCTCCGCTTTTTCT-3′), Gli1 (primers: 5′-TCCAATGACTCCACCACAAG-3′ and 5′-CAAAAGGGCAGACCAGAAAG-3′), VEGF (primers: 5′-CAACTTCTGGGCTCTTCTCG-3′ and 5′-CCTCTCCTCTTCCTTCTCTTCC-3′), and β-actin (primers: 5′-CCTCCTCCTGAGCGCAAGTA-3′ and 5′-GATGGAGGGGCCGGACT-3′) were analyzed with RT-qPCR. Reactions were performed according to the following protocol: initial denaturation at 95°C for 30 s, 40 cycles consisting of 95°C for 5 s, 60°C for 30 s, and 72°C for 30 s, and final elongation at 4°C for 5 min. The $2^{-\Delta\Delta CT}$ method was used to quantify the relative gene expression.

Western blot

The total protein was extracted according to the kit. Fifty micrograms of sample were loaded onto sodium dodecyl sulfate–polyacrylamide gels, separated using electrophoresis, and transferred to polyvinylidene fluoride (PVDF) membranes using standard procedures. After blocking with 5% skim milk and washing for 30 min with Tris buffered saline Tween (TBST), the PVDF membrane was immunoblotted with Smo antibody (1:1,000 dilution; ab72130; Abcam), Gli1 antibody (1:1,000 dilution; ab1515796; Abcam), VEGF antibody (1:500 dilution; sc7269; Santa Cruz), and β-actin antibody (1:2,000 dilution; Proteintech, Rosemont, IL, USA) overnight at 4°C. The membranes were then incubated with a horseradish peroxidase–conjugated anti-rabbit or anti-mouse immunoglobulin G secondary antibody.

Statistical analysis

SPSS 22.0 software was used for statistical analysis. All statistical data are expressed as mean ± standard deviation (SD). Difference test were analyzed using one-way analysis of variance. Least significant difference t-test was used for each two comparisons. $P < 0.05$ was considered significant.

Results

Quantitative assessment of retinal neovascularization using adenosine diphosphatase

The retinal vessels in the control group were mature. Large vessels were radially distributed from the optic disk to the periphery of the retina. The parapapillary diameter of retinal vessels was thick, and the vessel branches were regular without neovascularization (Figure 1A). Compared with the control group, there were a lot of angiogenesis and nonperfusion area from the OIR group (Figure 1B) and OIR-control group (Figure 1C). In the cyclopamine group, the avascular area, as well as the amount of angiogenesis, was reduced (Figure 1D). There were significant differences in the ratio of neovascularization and nonperfused area to the total retinal area (F=74.16, $P < 0.05$). The results of the quantitative analysis for each group are shown in Figure 1E.

Quantitative analysis of vascular endothelial cells

To confirm the inhibitory effect of cyclopamine, examination of 3.5 µm paraffin-processed cross-sections of mouse eyes was performed. Retinal vascular endothelial cell nuclei were rarely seen in the control group; the average cross-section was 4.00±0.63 (Figure 2A). The OIR and OIR-control groups had many retinal vascular endothelial cell nuclei in each cross-section, 24.87±3.48 (Figure 2B) and 26.43±3.45 (Figure 2C),
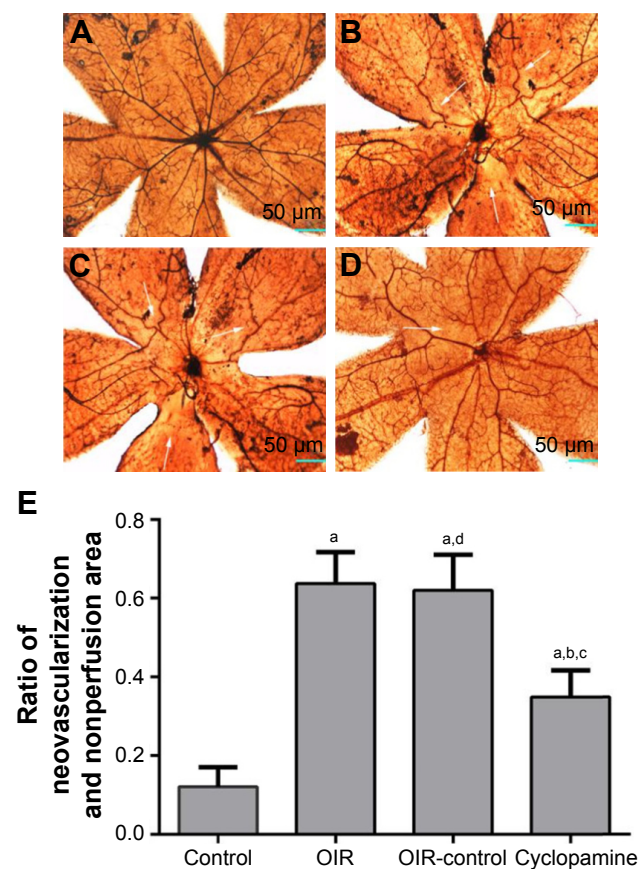
Figure 1 Inhibitory effect of cyclopamine on RNV in the OIR model.
Notes: Angiography using ADPase. The images are representative retinal angiographs from the eyes of control group (**A**), OIR group (**B**), OIR-control group (**C**), and cyclopamine group (**D**). The result of statistical analysis is illustrated in (**E**). The white arrows indicate neovascularization and nonperfusion region (magnification: 40×, bars: 50 μm). Three independent reviewers were blinded to grouping when counting the ratio of neovascularization and the area of nonperfusion region in order to assess severity of RNV. Data are shown as mean ± SD (n=10). [a]$P<0.05$ versus control group, [b]$P<0.05$ versus OIR group, [c]$P<0.05$ versus OIR-control group, [d]$P>0.05$ versus OIR group.
Abbreviations: ADPase, adenosine diphosphatase; OIR, oxygen-induced retinopathy; RNV, retinal neovascularization; SD, standard deviation.

Figure 2 Effect of cyclopamine on RNV in mice with OIR.
Notes: Preretinal neovascular cells were counted on 10 noncontinuous sections per eye, 10 eyes per group, and averaged. The images were representative retinal sections from the control group (**A**), OIR group (**B**), OIR-control group (**C**), and cyclopamine group (**D**). The statistical analysis result is illustrated in (**E**). The dark arrows indicate preretinal neovascular cells (magnification: 400×, bars: 50 μm). Three independent reviewers were blinded to grouping when counting the cells. Data are shown as mean ± SD (n=100). [a]$P<0.05$ versus control group, [b]$P<0.05$ versus OIR group, [c]$P<0.05$ versus OIR-control group, [d]$P>0.05$ versus OIR group.
Abbreviations: OIR, oxygen-induced retinopathy; RNV, retinal neovascularization; SD, standard deviation.

respectively. The number of retinal vascular endothelial cell nuclei in the cyclopamine group was obviously reduced; the average was 18.36±9.93 (Figure 2D). There was a significant difference among the four groups in the number of vascular endothelial cells in the retina (F=72.87, $P<0.05$). The results of the quantitative analysis for each group are shown in Figure 2E.

Immunohistochemical staining

Immunohistochemistry was performed to investigate the localization and expression levels of Smo, Gli1, and VEGF in the control group, OIR group, OIR-control group, and cyclopamine group. Figure 3 shows that Smo, Gli1, and VEGF expressions were weakly detected in the ILM, ganglion cell
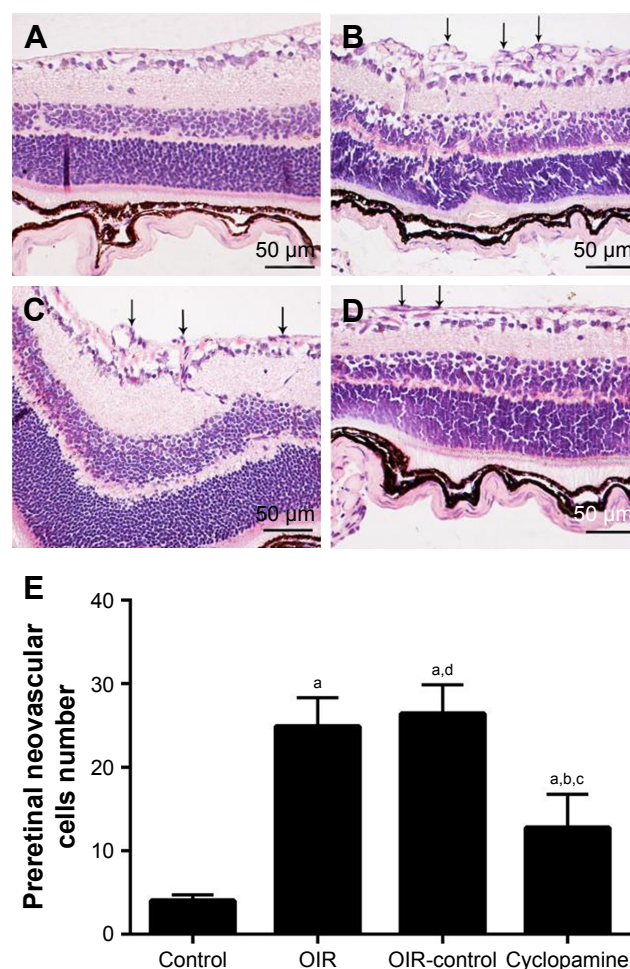
layer (GCL), and inner plexiform layer (IPL) of the control group. In the OIR and OIR-control groups, Smo and Gli1 were spread all over the retinal vessels, as well as the ILM, GCL, IPL, and inner nuclear layer. VEGF expression was widely distributed in almost all layers of the retina, and neovascularization had broken through the ILM. In the cyclopamine group, the target protein was significantly decreased, when compared with the OIR and OIR-control groups. A PBS-negative control had no brown granules. After immunohistochemical staining, the average optical density for each group was significant (F_{smo}=32.12, P_{smo}=0.00; F_{Gli1}=21.88, P_{Gli1}=0.00; F_{VEGF}=11.98, P_{VEGF}=0.001).
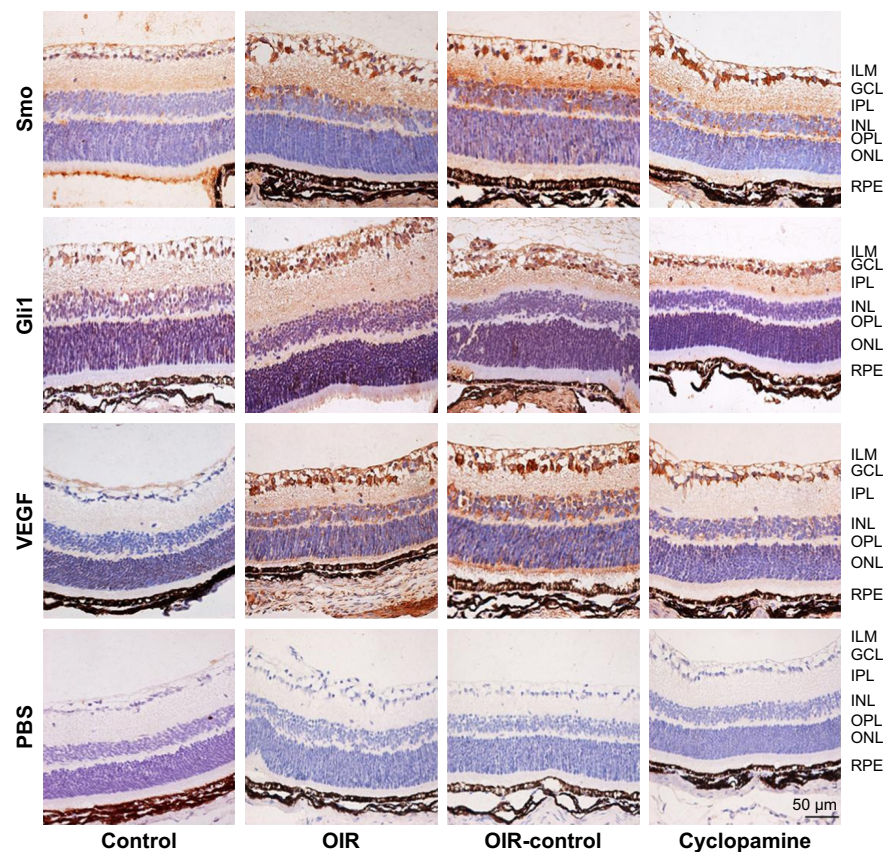
Figure 3 Smo, Gli1, and VEGF protein expressions were determined by immunohistochemistry (magnification, ×400, bar: 50 μm).
Abbreviations: GCL, ganglion cell layer; ILM, inner limiting membrane; INL, inner nuclear layer; IPL, inner plexiform layer; OIR, oxygen-induced retinopathy; ONL, outer nuclear layer; OPL, outer plexiform layer; PBS, phosphate buffer saline; RPE, retinal pigment epithelium; Smo, Smoothened; VEGF, vascular endothelial growth factor.

Expressions of Smo, Gli1, and VEGF mRNA

After reverse transcription–polymerase chain reaction, there was a significant difference in the relative expression of mRNA among the four groups (F_{smo}=43.33, P_{smo}=0.00; F_{Gli1}=130.12, P_{Gli}=10.00; F_{VEGF}=69.35, P_{VEGF}=0.00). The mRNA of Smo, Gli1, and VEGF in the control group demonstrated a weak positive expression, and the OIR and OIR-control groups demonstrated an enhanced trend compared with the control group; the expression of mRNA in the inhibitor group was higher than that of the control group. Figure 4 shows the expressions of Smo, Gli1, and VEGF for each group.

Expressions of Smo, Gli1, and VEGF protein

Western blot was used to detect the expressions of Smo, Gli1, and VEGF in the retinas of mice in the four groups (Figure 5A and B). There were significant differences in the relative expressions of Smo, Gli1, and VEGF protein in

each group (F_{smo}=15.65, P_{smo}=0.00; F_{Gli1}=14.99, P_{Gli1}=0.00; F_{VEGF}=30.10, P_{VEGF}=0.00). Three proteins were detected in the control group, indicating that the three target proteins are expressed during normal retinal development. The OIR and OIR-control groups were significantly upregulated. Use of the inhibitor, cyclopamine, can downregulate the expressions of Smo, Gli1, and VEGF protein.

Discussion

ROP is a proliferative vascular retinopathy; the main pathological changes include retinal vascular contraction, capillary degeneration, abnormal angiogenesis, vascular tortuosity, and abnormal retinal blood perfusion. It occurs after 32 weeks of gestation, with a birth weight of less than 1,500 g, along with a history of inhalation of a high oxygen concentration in premature infants or low birthweight infants. During the early stages of pregnancy, there are no blood vessels in the retina; the retinal blood vessels extend from the optic disk to the peripheral retina at 14–16 weeks, reach the nasal side of the limbus at about 36 weeks, and
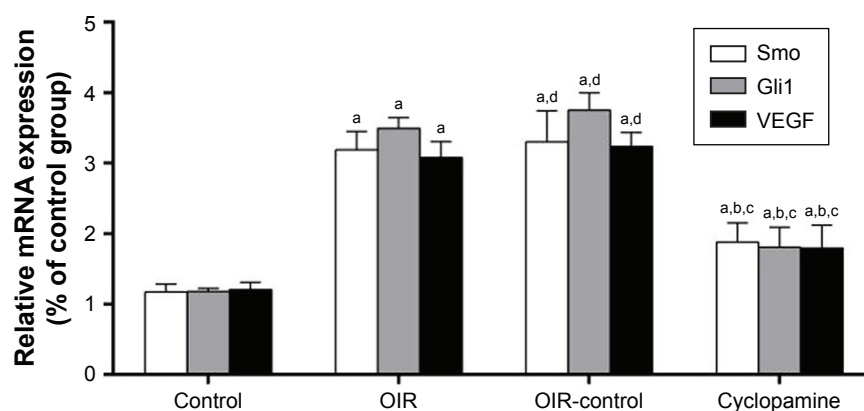
Figure 4 Cyclopamine inhibited RNV and VEGF through inhibition of the mRNA expression in hedgehog signaling pathway in the OIR mouse model.
Notes: Smo, Gli1, and VEGF were determined by RT-qPCR. Data are shown as mean ± SD (n=15). ^{a}P<0.05 versus control group, ^{b}P<0.05 versus OIR group, ^{c}P<0.05 versus OIR-control group, ^{d}P>0.05 versus OIR group.
Abbreviations: OIR, oxygen-induced retinopathy; RT-qPCR, real-time quantitative PCR; RNV, retinal neovascularization; Smo, Smoothened; VEGF, vascular endothelial growth factor.

reach the dentate margin at the end of 40 weeks. Because of the relative hypoxic environment of the uterus, the premature and immature retina continues to develop after birth, and the increasing of ambient oxygen content causes the normal growth of retinal vessels to be inhibited. The lack of nutrients from the normal blood vessels in the retina along with the gradually decreasing oxygen concentration leads to a relative lack of oxygen in the retina, thus stimulating pathological angiogenesis. Neovascularization is first seen in the retina that is known as retinal intraretinal microvascular abnormality (IRMA). With time, the new blood vessels will gradually grow into the vitreous cavity, called RNV.
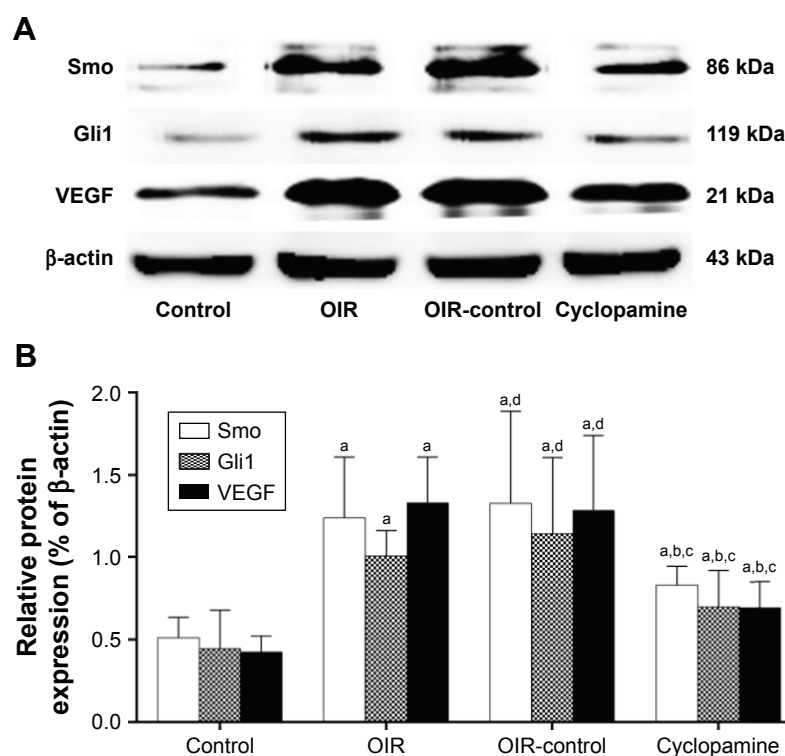

Figure 5 Smo, Gli1, and VEGF protein expressions and cyclopamine inhibited RNV through inhibition of the protein expression in Hedgehog signaling pathway in the OIR mouse model. (**A**) Western blot assay for protein expression. (**B**) Statistical analysis.
Notes: Protein expressions of Smo, Gli1, and VEGF were determined by Western blotting. Protein expressions were normalized to β-actin. Data are shown as mean ± SD (n=15). ^{a}P<0.05 versus control group, ^{b}P<0.05 versus OIR group, ^{c}P<0.05 versus OIR-control group, ^{d}P>0.05 versus OIR group.
Abbreviations: OIR, oxygen-induced retinopathy; RNV, retinal neovascularization; Smo, Smoothened; SD, standard deviation; VEGF, vascular endothelial growth factor.

Different from normal retinal blood vessels, IRMA and RNV cannot complete the functions of blood vessel walls, so plasma can penetrate the retina and vitreous cavity through blood vessel walls. The osmotic fluid destroys the stability of the inner environment of the retina, and the plasma components that infiltrate into the vitreous body can induce vitreous liquefaction, degeneration, fiber proliferation, and contraction. It can lead to serious complications such as a retinal hemorrhage and traction retinal detachment, which can impair vision.[4]

VEGF has an important role in the neovascularization process in ROP. VEGF is also known as vascular permeability factor or vasculotropin. VEGF has a key role in wound healing, tumor growth and metastasis, and embryo maturation.[5–7] It is involved in the regulation of the VEGF pathway and numerous factors. The trigger factors for VEGF in ischemia and hypoxia are key to produce VEGF; cells can generate a great amount of VEGF with hypoxia, which promotes vascular endothelial cell proliferation, migration, and maturation and increases vascular permeability.[8,9] VEGF is involved in the destruction of the blood–retinal barrier and continues throughout the disease. In recent years, it has been found that VEGF is an important factor in the pathogenesis of ROP, and anti-VEGF therapy has brought new hope for the improvement of retinal function in premature infants. Therefore, research on the mechanism of VEGF regulation and how to curtail the pathological development of VEGF has become an important issue.

Hedgehog signaling is widely found in vertebrates and invertebrates and is highly conserved. It has an important role in the growth and development of many organisms. The Hedgehog signaling pathway can regulate the occurrence of tumors and craniofacial development of animals and participate in the regulation of the homeostasis of the environment; if the signal pathway is inhibited, it can lead to a single eye deformity and a variety of diseases.[10–15] Recent studies have indicated that the Hedgehog signaling pathway is involved in the regulation of retinal ganglion cell (RGC) proliferation and neurite growth direction;[16–20] Muller cells promote glia maturation and differentiation,[21,22] regulate cone cells and rod cells in mitosis and proliferation activity,[23–26] and control the growth of retinal pigment epithelium cells regarding time and spatial location.[27–30] Hedgehog family is composed of Sonic hedgehog (Shh), Indian Hedgehog, and Desert Hedgehog in the vertebrate.[31] Shh is the first gene that can regulate the phenotype of RGC which promotes the production of RGC by regulating the critical role of Pax6 in the development of the eye.[32,33] Both Ptc and Smo are important receptors on the downstream target cell membrane of Hedgehog. Ptc is a 12-transmembrane protein, divided into Ptc1 and Ptc2 in the human body. The expression of Ptc1 is more extensive, as its function is to combine Hh and inhibit Smo. When the Hedgehog signal does not exist, Ptc1 combines with Smo to inhibit downstream signal transduction; when external factors activate Hedgehog signaling pathway, the inhibitory effect of Ptc1 on Smo will be relieved and the expression of downstream genes will enhance. Smo is a 7-transmembrane protein, which is a member of a G-protein-coupled receptor family and is a key factor in the intracellular transduction of signaling pathways, which activate downstream target genes. Gli (in Drosophila similar protein Ci) has a transcription factor function and is mainly localized in the nucleus and cytoplasm; the signals can be sent from one cell to another cell, activating target genes. Vertebrates have three nuclear transcription factors Gli1, Gli2, and Gli3 that perform their respective duties. Gli1 is the major transcription factor, which has a role in the transcriptional activation of target genes. Gli2 and Gli3 have an important role in activation or inhibition.[34]

The Hedgehog signaling pathway has a key role in the development of many ocular neovascular diseases, such as the cornea, choroid, and retina. Fujita et al found that the upregulated expression of Shh leads to corneal neovascularization in alkali burns in rats;[35] exogenous Shh promotes angiogenesis; and a local injection of the specific Hedgehog signaling pathway inhibitor membrane protein receptor, Smo, can shorten the length of peripheral blood vessels. Shh can enhance the formation of capillary endothelial cells in vitro through the VEGF signaling pathway.

Surace et al reported that the Shh pathway was activated in the retina in animal models of retinal and choroidal neovascularization.[36] The expressions of Ptc1 and Gli1 mRNAs were upregulated in choroidal neovascularization in laser-induced retinopathy. Area of neovascularization expanded after using agonist purmorphamine, and the inhibitor used, cyclopamine, could prevent an increase in Shh and decrease the formation of choroidal neovascularization.[37] Yao et al suggested that the Hedgehog signaling pathway is a target gene of platelet-derived growth factor BB (PDGF-BB), which can increase the expression of extracellular signal-regulated kinase 1/2 and Akt phosphorylation and thus participate in PDGF-BB-induced endothelial cell migration and recruitment.[38] It has been further demonstrated that the Hedgehog signaling pathway may be the key signaling pathway for ocular neovascularization.

Researchers found that the Hedgehog signaling pathway is involved in the regulation of VEGF in a variety of tumor

tissues and cells. Lin et al studied the pathogenesis of colorectal cancer and observed that with the use of the drug, Hedyotis diffusa Willd, the Hedgehog signaling pathway was inhibited, leading to a significant decrease in tumor microvessel density and VEGF-A, along with its specific receptor VEGFR2, suggesting that VEGF is the target gene pathway.[39] In pancreatic cancer, the expression of Embelin can inhibit vascular markers in cancer cell lines, COX-2, VEGF, VEGFR, and IL-8 by decreasing the amount of Shh protein, thus reducing cancer angiogenesis that can control the metastasis of cancer cells.[40] In cutaneous squamous cell carcinoma, Hh is involved in the proliferation and metastasis of cancer cells; Gli1 can significantly improve tumor incidence and multiplicity; and Smo, Gli1, and cyclopamine can inhibit VEGF expression, tumor invasion, and migration.[41] Hh is involved in the growth of human glioma. In both in vivo and in vitro experiments, we found that VEGF, matrix metalloproteinase-2 (MMP-2), and MMP-9 increased with the activation of Hedgehog signal pathway and decreased with the inhibition.[42] Hedgehog inhibitor GDC-0449 can decrease angiogenesis by decreasing the expression of VEGF-A in hepatocellular carcinoma.[43] In hypoxic ischemic diseases, the Hedgehog signaling pathway regulates the production of VEGF, which is involved in stress response after injury. The expressions of VEGF, Ang-1, Ang-2, and Shh signaling components are increased in astrocytes with oxygen–glucose deprivation. In addition, the expressions of VEGF, Ang-1, and Ang-2 can be decreased with Shh pathway inhibitors. Moreover, exogenous Shh can increase the expressions of VEGF, Ang-1, and Ang-2 through NR2F2.[44] Cardiac fibroblasts will release a large amount of Shh after ischemic injury that can upregulate the expressions of VEGF, SDF-1a, IGF-1, and Shh, thus preventing cellular degeneration. These results suggest that Shh can reduce ischemic tissue damage and promote tissue repair and regeneration.[45] In addition, the Hedgehog signaling pathway can regulate the self-renewal and differentiation of hematopoietic stem cells through VEGF.[46] In embryonic stem cells, Shh can increase reepithelialization and VEGF expression in skin wounds, thus increasing the wound-healing ability of mice.[47] Hedgehog regulates the formation of intersegmental vessels through the VEGF signaling pathway.[48]

With the establishment of a variety of animal models on angiogenesis, we have a greater understanding of RNV. The OIR model is used widely.[49] The structure of the mouse retina is similar to that of human retinal blood vessels, meaning that the retinal blood vessels move toward the retinal surface. From the superficial vascular network to the deep retina, the middle and deep retinal vascular networks were formed. The OIR model was used to simulate the formation of ROP. Thus, the occurrence of ROP is based on the immature retinal vascular system and its response to changes in oxygen concentration. In this paper, changes in oxygen concentration during growth after birth were used to simulate ROP and to explore changes in VEGF in the Hedgehog signaling pathway.

The aim of this study was to investigate the relationship between Smo, Gli1, VEGF, and RNV in Hedgehog signaling pathway. The results showed that under normal oxygen concentrations in retinal tissue, Smo, Gli1, and VEGF had a low expression of transcription and protein level; high oxygen induced Smo, Gli1, and VEGF expressions significantly and increased RNV; a large nonperfused area was apparent; cyclopamine could inhibit Smo, Gli1, and VEGF expressions and alleviate ischemia and hypoxia but could not completely curtail retinal damage. The specific reaction necessitates additional study. Thus, we hypothesized that the Hedgehog signaling pathway is involved in the regulation of VEGF in ROP that may be an important regulatory signal involved in retinal physiology and pathology. Inhibition of the Hedgehog signaling pathway may provide a new therapeutic approach for the treatment of ROP.

Acknowledgment

Disclosure
The authors report no conflicts of interest in this work.

References
1. Promelle V, Milazzo S. Retinopathy of prematurity. *J Fr Ophthalmol*. 2017;40(5):430–437.
2. Korzh VP. Multiple role of hedgehog genes in vertebrates: data from analysis of mutations. *Ontogenez*. 1998;29(5):323–334.
3. Smith LE, Wesolowski E, McLellan A, et al. Oxygen-induced retinopathy in the mouse. *Invest Ophthalmol Vis Sci*. 1994;35(1):101–111.
4. Sapieha P, Joyal JS, Rivera JC, et al. Retinopathy of prematurity: understanding ischemic retinal vasculopathies at an extreme of life. *J Clin Invest*. 2010;120(9):3022–3032.
5. Chen J, Sun X, Shao R, Xu Y, Gao J, Liang W. VEGF siRNA delivered by polycation liposome-encapsulated calcium phosphate nanoparticles for tumor angiogenesis inhibition in breast cancer. *Int J Nanomedicine*. 2017;21(12):6075–6088.
6. Duloquin L, Lhomond G, Gache C. Localized VEGF signaling from ectoderm to mesenchyme cells controls morphogenesis of the sea urchin embryo skeleton. *Development*. 2007;134(12):2293–2302.
7. Lai PX, Chen CW, Wei SC, et al. Ultrastrong trapping of VEGF by graphene oxide: anti-angiogenesis application. *Biomaterials*. 2016;109: 12–22.
8. Yang X, Zhu H, Ge Y, et al. Melittin enhances radiosensitivity of hypoxic head and neck squamous cell carcinoma by suppressing HIF-1α. *Tumour Biol*. 2014;35(10):10443–10448.

9. Ma DH, Chen HC, Lai JY, et al. Matrix revolution: molecular mechanism for inflammatory corneal neovascularization and restoration of corneal avascularity by epithelial stem cell transplantation. *Ocul Surf*. 2009;7(3):128–144.

10. Rimkus TK, Carpenter RL, Qasem S, Chan M, Lo HW. Targeting the Sonic Hedgehog Signaling Pathway: Review of Smoothened and GLI Inhibitors. *Cancers (Basel)*. 2016;8(2):1–78.

11. Xavier GM, Seppala M, Barrell W, Birjandi AA, Geoghegan F, Cobourne MT. Hedgehog receptor function during craniofacial development. *Dev Biol*. 2016;415(2):198–215.

12. Christ A, Herzog K, Willnow TE. LRP2, an auxiliary receptor that controls sonic hedgehog signaling in development and disease. *Dev Dyn*. 2016;245(5):569–579.

13. Zhou D, Tan RJ, Liu Y. Sonic hedgehog signaling in kidney fibrosis: a master communicator. *Sci China Life Sci*. 2016;59(9):920–929.

14. Matz-Soja M, Rennert C, Schönefeld K, et al. Hedgehog signaling is a potent regulator of liver lipid metabolism and reveals a GLI-code associated with steatosis. *Elife*. 2016;17(5):1–81.

15. Gao H, Wang D, Bai Y, et al. Hedgehog gene polymorphisms are associated with the risk of Hirschsprung's disease and anorectal malformation in a Chinese population. *Mol Med Rep*. 2016;13(6):4759–4766.

16. Fabre PJ, Shimogori T, Charron F. Segregation of ipsilateral retinal ganglion cell axons at the optic chiasm requires the Shh receptor Boc. *J Neurosci*. 2010;30(1):266–275.

17. Gordon L, Mansh M, Kinsman H, Morris AR. Xenopus sonic hedgehog guides retinal axons along the optic tract. *Dev Dyn*. 2010;239(11):2921–2932.

18. Guo D, Standley C, Bellve K, Fogarty K, Bao ZZ. Protein kinase Cα and integrin-linked kinase mediate the negative axon guidance effects of Sonic hedgehog. *Mol Cell Neurosci*. 2012;50(1):82–92.

19. StacherHörndli C, Chien CB. Sonic hedgehog is indirectly required for intraretinal axon pathfinding by regulating chemokine expression in the optic stalk. *Development*. 2012;139(14):2604–2613.

20. Kolpak A, Zhang J, Bao ZZ. Sonic hedgehog has a dual effect on the growth of retinal ganglion axons depending on its concentration. *J Neurosci*. 2005;25(13):3432–3441.

21. McNeill B, Perez-Iratxeta C, Mazerolle C, et al. Comparative genomics identification of a novel set of temporally regulated hedgehog target genes in the retina. *Mol Cell Neurosci*. 2012;49(3):333–340.

22. Todd L, Fischer AJ. Hedgehog signaling stimulates the formation of proliferating Müller glia-derived progenitor cells in the chick retina. *Development*. 2015;142(15):2610–2622.

23. Stenkamp DL, Frey RA, Prabhudesai SN, et al. Function for Hedgehog genes in zebrafish retinal development. *Dev Biol*. 2002;225(3):344–350.

24. Pillai-Kastoori L, Wen W, Wilson SG, et al. Sox11 is required to maintain proper levels of Hedgehog signaling during vertebrate ocular morphogenesis. *PLoS Genet*. 2014;10(7):1–19.

25. Amirpour N, Karamali F, Rabiee F, et al. Differentiation of human embryonic stem cell-derived retinal progenitors into retinal cells by Sonic hedgehog and/or retinal pigmented epithelium and transplantation into the subretinal space of sodium iodate-injected rabbits. *Stem Cells Dev*. 2012;21(1):42–53.

26. Dakubo GD, Mazerolle C, Furimsky M, et al. Indian hedgehog signaling from endothelial cells is required for sclera and retinal pigment epithelium development in the mouse eye. *Dev Biol*. 2008;320(1):242–255.

27. Yoshikawa T, Mizuno A, Yasumuro H, et al. MEK-ERK and heparin-susceptible signaling pathways are involved in cell-cycle entry of the wound edge retinal pigment epithelium cells in the adult newt. *Pigment Cell Melanoma Res*. 2012;25(1):66–82.

28. Kobayashi T, Yasuda K, Araki M. Coordinated regulation of dorsal bone morphogenetic protein 4 and ventral Sonic hedgehog signaling specifies the dorso-ventral polarity in the optic vesicle and governs ocular morphogenesis through fibroblast growth factor 8 upregulation. *Dev Growth Differ*. 2010;52(4):351–363.

29. Perron M, Boy S, Amato MA, et al. A novel function for Hedgehog signalling in retinal pigment epithelium differentiation. *Development*. 2003;130(8):1565–1577.

30. Spence JR, Madhavan M, Ewing JD, Jones DK, Lehman BM, Del Rio-Tsonis K. The hedgehog pathway is a modulator of retina regeneration. *Development*. 2004;131(18):4607–4721.

31. Lin YC, Roffler SR, Yan YT, Yang RB. Disruption of scube2 impairs endochondral bone formation. *J Bone Miner Res*. 2015;30(7):1255–1267.

32. Kayama M, Kurokawa MS, Ueda Y, et al. Transfection with pax6 gene of mouse embryonic stem cells and subsequent cell cloning induced retinal neuron progenitors, including retinal ganglion cell-like cells, in vitro. *Ophthalmic Res*. 2010;43(2):79–91.

33. Manuel M, Pratt T, Liu M, Jeffery G, Price DJ. Overexpression of Pax6 results in microphthalmia, retinal dysplasia and defective retinal ganglion cell axon guidance. *BMC Dev Biol*. 2008;8(59):1–21.

34. Robbins DJ, Hebrok M. Hedgehogs: la dolce vita. Workshop on hedgehog-Gli signaling in cancer and stem cells. *EMBO Rep*. 2007;8(5):451–455.

35. Fujita K, Miyamoto T, Saika S. Sonic hedgehog: its expression in a healing cornea and its role in neovascularization. *Mol Vis*. 2009;15:1036–1044.

36. Surace EM, Balaggan KS, Tessitore A, et al. Inhibition of ocular neovascularization by hedgehog blockade. *Mol Ther*. 2006;13(3):573–579.

37. Nochioka K, Okuda H, Tatsumi K, Morita S, Ogata N, Wanaka A. Hedgehog signaling components are expressed in choroidal neovascularization in laser-induced retinal lesion. *Acta Histochem Cytochem*. 2016;49(2):67–74.

38. Yao Q, Renault MA, Chapouly C, et al. Sonic hedgehog mediates a novel pathway of PDGF-BB-dependent vessel maturation. *Blood*. 2014;123(15):2429–2437.

39. Lin J, Wei L, Shen A, et al. Hedyotis diffusa Willd extract suppresses Sonic hedgehog signaling leading to the inhibition of colorectal cancer angiogenesis. *Int J Oncol*. 2013;42(2):651–656.

40. Huang M, Tang SN, Upadhyay G, et al. Embelin suppresses growth of human pancreatic cancer xenografts, and pancreatic cancer cells isolated from KrasG12D mice by inhibiting Akt and Sonic hedgehog pathways. *PLoS One*. 2014;9(4):1–10.

41. Sun Q, Bai J, Lv R. Hedgehog/Gli1 signal pathway facilitates proliferation, invasion, and migration of cutaneous SCC through regulating VEGF. *Tumour Biol*. 2016;10:16215–16225.

42. Cui D, Chen X, Yin J, Wang W, Lou M, Gu S. Aberrant activation of Hedgehog/Gli1 pathway on angiogenesis in gliomas. *Neurol India*. 2012;60(6):589–596.

43. Pinter M, Sieghart W, Schmid M, et al. Hedgehog inhibition reduces angiogenesis by downregulation of tumoral VEGF-A expression in hepatocellular carcinoma. *United European Gastroenterol J*. 2013;1(4):265–275.

44. Li Y, Xia Y, Wang Y, et al. Sonic hedgehog (Shh) regulates the expression of angiogenic growth factors in oxygen-glucose-deprived astrocytes by mediating the nuclear receptor NR2F2. *Mol Neurobiol*. 2013;47(3):967–975.

45. Johnson NR, Wang Y. Controlled delivery of sonic hedgehog morphogen and its potential for cardiac repair. *PLoS One*. 2013;8(5):1–6.

46. Crisan M, Solaimani Kartalaei P, Neagu A, et al. BMP and hedgehog regulate distinct AGM hematopoietic stem cells ex vivo. *Stem Cell Reports*. 2016;6(3):383–395.

47. Suh HN, Han HJ. Sonic hedgehog increases the skin wound-healing ability of mouse embryonic stem cells through the microRNA 200 family. *Br J Pharmacol*. 2015;172(3):815–828.

48. Moran CM, Myers CT, Lewis CM, Krieg PA. Hedgehog regulates angiogenesis of intersegmental vessels through the VEGF signaling pathway. *Dev Dyn*. 2012;241(6):1034–1042.

49. Grossniklaus HE, Kang SJ, Berglin L. Animal models of choroidal and retinal neovascularization. *Prog Retin Eye Res*. 2010;29(6):500–519.